Molecular Crystals and Liquid Crystals

ISSN: 1542-1406 (Print) 1563-5287 (Online) Journal homepage: http://www.tandfonline.com/loi/gmcl20

Pyrene bisiminopyridine ligand and its zinc complex

Awatef Ayadi, Diana Branzea, Haluk Dinçalp, Nabil Zouari & Abdelkrim El-Ghayoury

To cite this article: Awatef Ayadi, Diana Branzea, Haluk Dinçalp, Nabil Zouari & Abdelkrim El-Ghayoury (2016) Pyrene bisiminopyridine ligand and its zinc complex, Molecular Crystals and Liquid Crystals, 628:1, 188-197, DOI: 10.1080/15421406.2015.1137386

To link to this article: http://dx.doi.org/10.1080/15421406.2015.1137386

Published online: 13 May 2016.

MOL. CRYST. LIQ. CRYST.
2016, VOL. 628, 188–197
http://dx.doi.org/10.1080/15421406.2015.1137386

Taylor & Francis
Taylor & Francis Group

Pyrene bisiminopyridine ligand and its zinc complex

Awatef Ayadi[a,b], Diana Branzea[a], Haluk Dinçalp[c], Nabil Zouari[b], and Abdelkrim El-Ghayoury[a]

[a]Université d'Angers, CNRS UMR 6200, Laboratoire MOLTECH-Anjou, Angers Cedex, France; [b]Laboratoire de Physico-chimie de l'état solide, Université de Sfax, Route de Soukra, Sfax, Tunisia; [c]Department of Chemistry, Faculty of Arts and Science, Celal Bayar University, Muradiye-Manisa, Turkey

ABSTRACT

The synthesis of a pyrene bisiminopyridine ligand **L** was successfully accomplished by condensation between 1-aminopyrene and 2,6-pyridinecarboxaldehyde. The complexation of **L** with zinc triflate afforded a neutral metal complex formulated as $[Zn(H_2O)LCF_3SO_3)_2].2Et_2O$. In the complex, the ligand is coordinated to zinc(II) through its three nitrogen atoms which form a distorted octahedral environment together with three oxygen atoms, two from the triflate anions and one from aqua ligand. Both compounds have been characterized using NMR, elemental analysis, mass spectrometry, electronic absorption (UV-Vis) and infrared. Luminescence properties of these compounds show an emission maxima at 412 nm, indicating a pyrene monomer emission.

KEYWORDS

Pyrene; Iminopyridine; UV-Visible spectroscopy; Fluorescence; X-ray diffraction

1. Introduction

Polycyclic aromatic hydrocarbons such as pyrene represent the focus of intense research for a long time. As its large delocalization of π-electrons in pyrene offers distinctive optical/luminescence properties. Pyrene is a strongly hydrophobic compound dissolves in water with a concentration up to about 10^{-6} mol dm^{-3} at room temperature [1]. Pyrene based compounds attract notable attention because of their chemical stability as well as their large planar π-conjugated surface of pyrene generating a high fluorescence and are being extensively studied for various applications such as preparation of chemosensors [2]. In fact pyrene can be regarded as one of the most useful sensing molecules because it may emit as a monomer near 370–380 nm or as an excimer near 480 nm [3]. In particular, ongoing research for the design of such fluorescent chemosensors consists of covalently grafting one or multiple fluorophores onto a coordinating unit that can bind metal cations [4]. For example pyrene-bipyridine ligands and their corresponding metal complexes,[5] pyrene-terpyridine,[6] pyrene-hydroxamate, [7] pyrene-ethynyl [8] and pyrene-salicylidenes [9]. It has found use as active material for organic electronics applications such as OFETs, OLEDs and more recently as donor component in organic solar cells (OSCs) [10]. Pyridine based Schiff bases ligands such as 2,6-bis(imino)pyridyl, with their chelating abilities, form stable complexes, with various transition metals and are extensively used as catalysts for olefin polymerization [11].

CONTACT Abdelkrim El-Ghayoury abdelkrim.elghayoury@univ-angers.fr
Color versions of one or more of the figures in the article can be found online at www.tandfonline.com/gmcl.

In order to obtain new transition metal complexes with original structural and optical properties, we report herein the synthesis of the $Pyre_2$-BisIm-Py (L) that can act as an (N,N,N) pincer. This ligand has been obtained by the condensation reaction between 1-aminopyrene and 2,6-diformylpyridine. The reaction of this tridentate ligand (L) with zinc metal cation afforded a new fluorescent metal complex.

2. Experimental section

2.1. Materials

All manipulations were performed in air using commercial grade solvents. 1-aminopyrene, 2,6-pyridinedicarboxaldehyde and zinc triflate were of reagent grade quality and used as received.

2.2. Instrumentation

^{1}H and ^{13}C NMR were recorded on a Bruker 300 MHz spectrometer. The measurements were performed in $CDCl_3$ and tetramethylsilane (TMS) was used as internal standard. The following abbreviations are used to represent the multiplicity of the signals: s (singlet), d (doublet), the spin spin coupling constants (J) were measured. Infrared spectra were recorded on a Bruker vertex 70 spectrometer, the measurements were recorded in the 400 to 4000 cm^{-1} range. Elemental analyses (C, H and N) were performed on a Thermo-Scientific Flash 2000 Organic. Mass spectrometry measurements were performed on a Bruker Biflex-III TM which uses 1,8,9-trihydroxyanthracene as matrix. UV-visible spectra were recorded at room temperature in quartz cuvettes using Perkin Elmer spectrophotometer. Fluorescence and life time measurements were recorded on a FLSP 920 Edinburg fluorescence phosphorescence spectrophotometer. The excitation wavelength was set to 317 nm for solution measurements. Quantum yields of fluorescence were measured by comparing the fluorescence intensity of the sample to that of the optically dilute solutions of pyrene standard. Melting points were determined with a Melting Point Apparatus SMP3.

2.3. Synthesis

2.3.1. Synthesis of (E)-N-((6-((E)-(pyren-2-ylimino)pyridin-2-yl)methylene)pyren-1-amine L

1-Aminopyrene (0.200 g, 0.92 mmol) and 2,6-pyridinecarboxaldehyde (0.062 g, 0.46 mmol) were dissolved in ethanol (20 mL), three drops of acetic acid were added and the reaction mixture was refluxed overnight. After cooling to room temperature, a yellow precipitate was formed which was filtered and washed with additional ethanol and dried to afford a yellow powder of ligand **L** (0.232 g, 94%). M.p.: 290°C.^{1}H-NMR (300 MHZ, $CDCl_3$) δ/ppm: 9.06 (s, 2H), 8.82 (d, 2H, J = 9.1 Hz), 8.70 (d, 2H, J = 7.7 Hz), 8.24 (m, 9H), 8.12 (s, 4H), 8.06 (t, 2H, J = 7.5 Hz), 7.95 (d, 2H, J = 8.1 Hz).^{13}C-NMR (75 MHz, $CDCl_3$) δ/ppm: 151.9, 146.1, 138.7, 138, 131.4, 127.4, 126.2, 125.6, 125.3, 125.3, 125.2, 120.1, 111.4, 111.2. Anal. Calcd for $C_{39}H_{23}N_3$: C, 87.77%; H, 4.31%; N, 7.87% Found: C, 87.28%; H, 4.17%; N, 7.62%. MALDI-TOF MS calcd: m/z = 533.18 Da. found: m/z = 534.4 $[M]^+$. HR-MS (M): for $C_{39}H_{23}N_3$: 533.1892. Found 533.1885. Selected IR bands (cm-1): ν = 3036, 1594, 1565, 1448, 1306, 1182, 829, 705, 675, 613, 600.

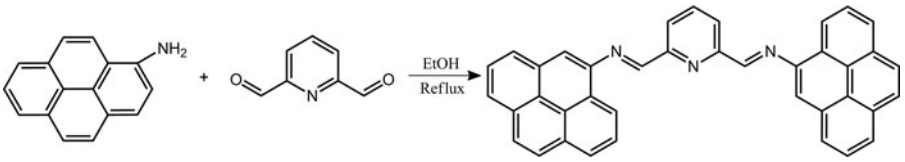

Scheme 1. Synthetic scheme of the $Pyre_2$-BisIm-Py (**L**).

2.3.2. Synthesis of zinc complex 1

Ligand **L** (0.010 g, 0.018 mmol) in CH_2Cl_2 (5 mL) was reacted with a half equivalent of zinc triflate (0.0034 g, 0.009 mmol) in CH_3CN (3 mL). The mixture was sonicated for 3 min and on top of this solution, diethyl ether was added which led to the formation of good quality single crystals of zinc complex after three weeks. Yield: 55%. M.p.: 230–235°C.^{1}H-NMR (300 MHZ, $CDCl_3$) δ/ppm: 8.87 (s, 2H), 8.59 (m, 2H), 8.13 (m, 18H), 3.49 (q, 8H, J = 6.99 Hz, J = 7.01 Hz), 2.02 (s, 2H), 1.22 (t, 12H, J = 7.02 Hz). MALDI-TOF MS for $(ZnL(SO_3CF_3)_2$ calcd: m/z = 895.02, found: m/z = 895.6. Selected IR bands (cm-1): ν = 2974, 2352, 1586, 1470, 1302, 1215, 1166, 1091, 1018, 839, 636, 512.

3. Results and discussion

3.1. Synthesis and characterization

The protocol followed for the synthesis of the new (E)-N-((6-((E)-(pyren-2-ylimino)pyridin-2-yl)methylene)pyren-1-amine pincer (**L**, $Pyre_2$-BisIm-Py) is presented in (Scheme 1). It was obtained in a good yield by the condensation reaction between 1-aminopyrene and 2,6-diformylpyridine [12].

This tridentate ligand was reacted with a half equivalent of zinc triflate $[Zn(SCF_3O_3)_2]$ in a dicloromethane/acetonitrile solvents mixture to afford good quality single crystals of $[Zn(H_2O)L(CF_3SO_3)_2].2Et_2O$ (Scheme 2) that were suitable for the X-ray crystal structure determination.

Crystal structure description

Experimental X-ray diffraction data on single crystals were collected at room temperature using a Bruker Nonius Kappa CCD diffractometer operating with a Mo-Kα (λ = 0.71073 Å) X-ray tube with a graphite monochromator. The structures were solved by direct methods and

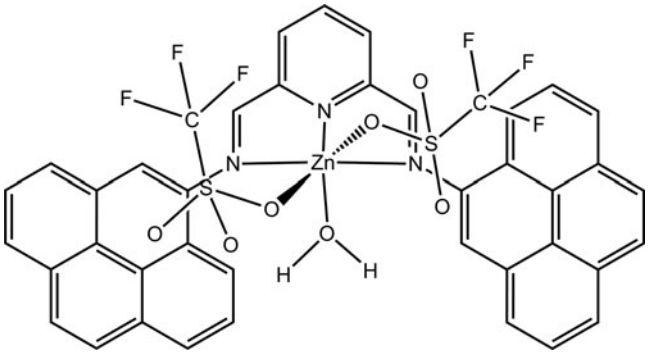

Scheme 2. Chemical structure of zinc complex.

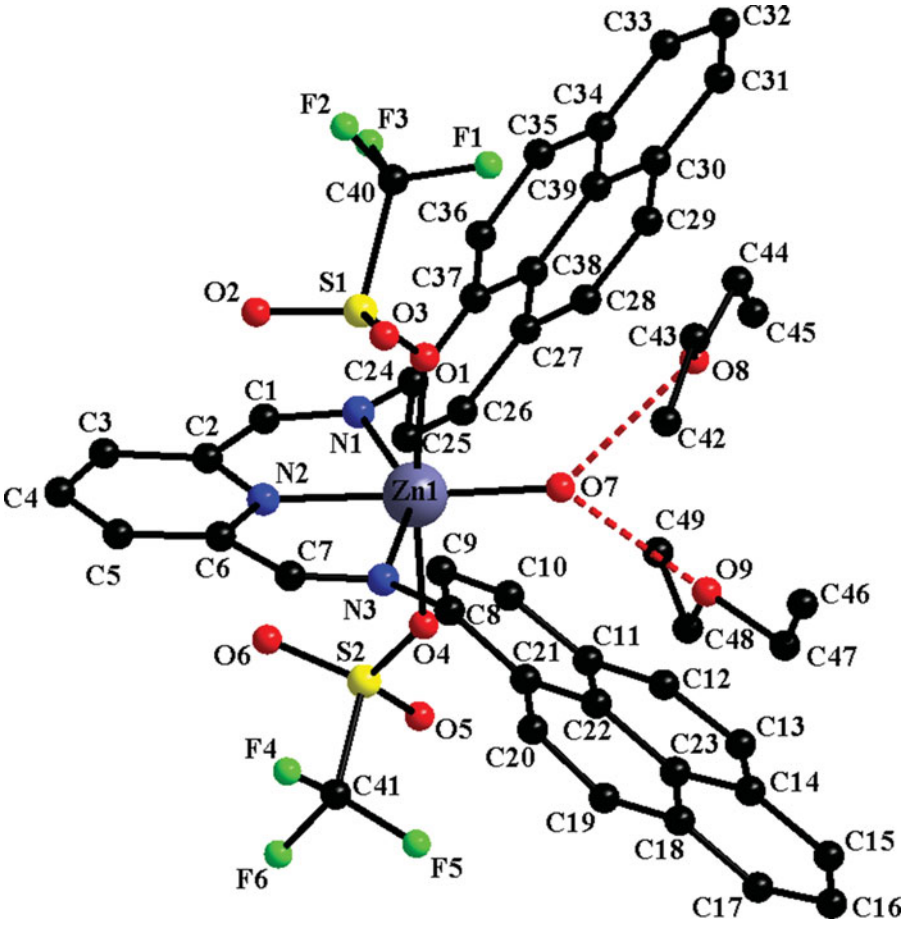

Figure 1. Crystal structure of complex with atom numbering scheme. Hydrogen atoms were omitted for clarity.

refined (SHELXL-97) by full-matrix least-square procedures on F^2 [13]. All non-H atoms of the molecules were refined anisotropically, and hydrogen atoms were introduced at calculated positions (riding model), included in structure factor calculations but not refined. Crystallographic data for the structural analysis have been deposited within the Cambridge Crystallographic Data Centre, CCDC 1403835.

Single crystals of complex were obtained *via* slow diffusion of diethyl ether into a dichloromethane/acetonitrile mixture, and the crystal structure was determined using single crystal X-ray diffraction analysis confirming the proposed formula of the complex (Figure 1), selected parameters of the X-ray diffraction data collection and refinement are gathered in Table 1. The relevant bond and angle parameters are summarized in Table 2.

In complex **1**, the tridentate **L** ligand is coordinated to the zinc(II) in a bis-chelating manner through its three nitrogen atoms which form a distorted octahedral environment together with three oxygen atoms, two from the triflate anions and the third provided by an aqua ligand. The distortion of the octahedral geometry around the Zn(II) ion is caused by the specific requirements of the bis-chelating ligand with small bite angles (N1–Zn1–N2 75.45(9)° and N2–Zn1–N3 74.76(9)°). The Zn1–N1(pyridyl) bond (Zn1–N2 2.042(2) Å) is shorter than the Zn1–N(imino) bonds (Zn1–N1 2.298(2) and Zn1–N3 2.350(2) Å) and the formal double bond character in the imino fragments is maintained (C1–N1 1.268(4) Å and C7–N3 1.274(4)

Table 1. Crystal data and structure refinement for complex **1**.

compound	Complex1
empirical formula	$C_{49}H_{45}F_6N_3O_9S_2Zn$
fw	1063.37
T (K)	293(2)
wavelength (Å)	0.71073
crystsyst	triclinic
space group	*P* −1
a (Å)	12.2371(8)
b (Å)	13.9579(17)
c (Å)	14.3613(5)
α(deg)	85.773(5)
β(deg)	87.184(4)
γ(deg)	86.845(8)
V (Å^3)	2440.1(3)
Z	2
D_c (g cm^{-3})	1.447
abs coeff (mm^{-1})	0.670
F(000)	1096
cryst size (mm^3)	0.25 × 0.2 × 0.15
θ range for data collection (deg)	1.67–29.15
reflns collected	12573
indepreflns	7981
completeness (%)	99.0
refinement method	full-matrix least squares on F^2
data/restraints/param	12573/0/638
GOF on F^2	1.032
final *R* indices [$I > 2\sigma(I)$]	R1 = 0.0523, wR2 = 0.1067
R indices (all data)	R1 = 0.1092, wR2 = 0.1377
largest diff. peak and hole (e Å^{-3})	0.645 and –0.473

Å). In the **L** ligand, the dihedral angles between the least-square planes of the pyrene fragments and NN-chelate imine-pyridine fragment are of 57.16° and 71.55°.

Analyzing the crystal packing of **1** numerous intra- and intermolecular interactions are observed, the geometric parameters of these contacts are gathered in table 3. Within the molecule of **1** hydrogen bonds are established between oxygen or fluorine atoms from the coordinated triflate anions and vicinal hydrogen atoms of the pyrene fragment. The aqua ligand also forms two hydrogen bonds with two crystallization molecules of diethyl ether.

Apart from the intramolecular interactions, the molecules of **1** are interconnected *via* hydrogen bonds into layers parallel to the *ac* crystallographic plane as depicted in figure 2.

Table 2. Hydrogen bonding geometry (distances in Å and angles in °) in complex **1**.

bond length (Å)			
N1—Zn1	2.298(2)	O1—Zn1	2.192(2)
N2—Zn1	2.042(2)	O4—Zn1	2.159(2)
N3—Zn1	2.350(2)	C1—N1	1.268(4)
O7—Zn1	1.950(2)	C7—N3	1.274(4)
angle values (°)			
O7—Zn1—N2	176.84(11)	O4—Zn1—N1	85.70(8)
O7—Zn1—O4	88.27(11)	O1—Zn1—N1	93.21(8)
N2—Zn1—O4	94.40(9)	O7—Zn1—N3	103.26(11)
O7—Zn1—O1	85.18(11)	N2—Zn1—N3	74.76(9)
N2—Zn1—O1	92.24(8)	O4—Zn1—N3	97.31(9)
O4—Zn1—O1	172.77(8)	O1—Zn1—N3	87.19(8)
O7—Zn1—N1	106.46(11)	N1—Zn1—N3	150.20(9)
N2—Zn1—N1	75.45(9)	C1—N1—Zn1	110.05(19)

Table 3. Hydrogen bonding geometry (distances in Å and angles in °) in complex **1**.

D–H···A	d(D···H)	d(H···A)	d(D ···A)	<(DHA)	
O7–H7A···O9^{i}	0.72	2.03	2.7506(48)	168.91	*
O7–H7B···O8^{i}	0.72	2.06	2.7702(40)	164.17	*
O7–H7B···O1^{i}	0.72	2.64	2.8089(34)	95.58	*
C36–H36···O1^{i}	0.93	2.65	3.4808(35)	148.63	??
C9–H9···O3^{i}	0.93	2.73	3.3299(53)	122.27	*
C20–H20···O4^{i}	0.92	2.56	3.4285(41)	155.46	*
C3–H3···O6^{ii}	0.93	2.39	3.3108(43)	169.07	
C4–H4···O3^{iii}	0.92	2.70	3.3814(48)	129.81	
C5–H5···O2^{iii}	0.93	2.42	3.3001(43)	157.29	
C10–H10···O5^{iv}	0.92	2.72	3.5718(45)	151.91	
C16–H16···O2i^{iv}	0.93	2.64	3.3694(51)	135.43	
C26–H26···O3^{v}	0.93	2.70	3.5402(44)	150.35	
C13–H13···F4^{vi}	0.93	2.66	3.1818(56)	115.68	
C35–H35···F2^{vii}	0.92	2.65	3.5384(42)	160.07	
C36–H36···F3^{i}	0.93	2.61	3.3123(36)	131.87	*

Symmetry transformations used to generate atoms:
i) x, y, z; ii) -x, 1-y, -z; iii) 1-x, 1-y, -z; iv) x, y, 1+z; v) −1+x, y, z; vi) 1-x, 1-y, 1-z; vii) 1-x, -y, -z.
* intramolecular interactions

Within these layers π-π stacking between the aromatic rings from the pyrene units (Cg1··· Cg2 3.84 Å, where Cg1 and Cg2 are the centers of gravity of the C8÷C11/C21/C22 and C18÷C23 rings) of neighboring molecules also sustain the solid state structure.

Finally, π-π interactions established also between the adjacent pyrene fragments (the pyrene fragments overlap only partially, Cg3··· Cg4 3.83 Å and Cg5···Cg6 3.80 Å, where Cg3, Cg4, Cg5 and Cg6 are the centers of gravity of the C24÷C27/C37/C8, C30÷C34/C39,

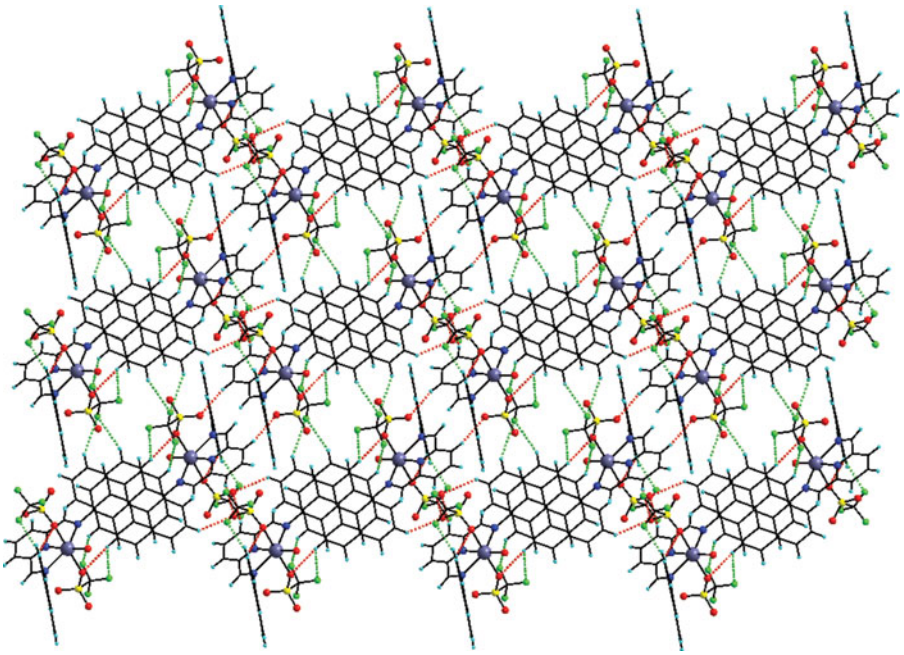

Figure 2. Perspective view of a supramolecular sheet generated via hydrogen bonds (H···O in red dashed lines and H···F in green dashed lines).

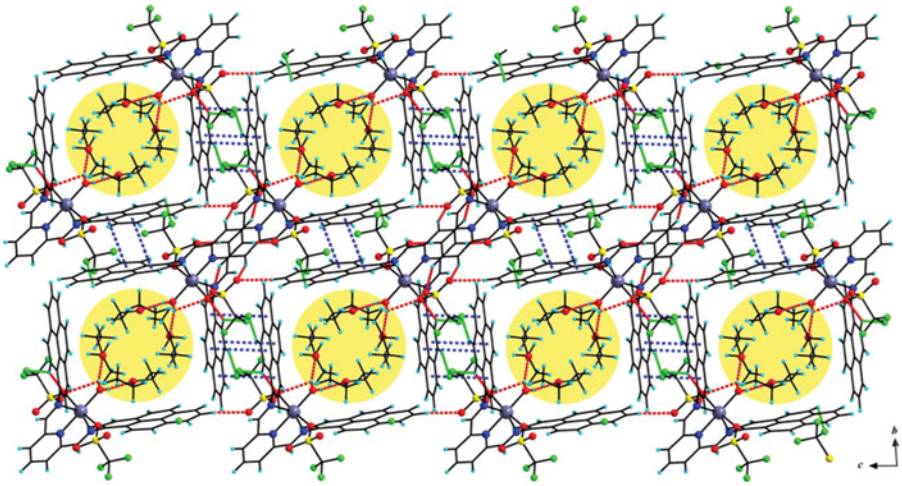

Figure 3. Crystal packing in **1**: hydrogen bonds and π-π stacking (blue dashed lines) interactions linking the molecules to form a 3D network with channels filled by diethyl ether crystallization solvent molecules (highlighted in yellow).

C27÷C30/C38/C39 and, C34÷C39 rings, respectively) act as zippers for the molecules belonging to neighboring sheets constructing a 3D supramolecular net with channels filled by crystallization solvent molecules (figure 3).

3.2. Optical properties

Figure 4 shows the UV-Visible absorption spectra of ligand **L** and the zinc complex **1** that were recorded in dichloromethane solution ($\sim 2{\cdot}8{*}10^{-5}$M) at room temperature. Ligand **L** gives characteristic intraligand (IL) $\pi \rightarrow \pi*$ and $n \rightarrow \pi*$ transitions around 364 and 384 nm with a weak shoulder around 415 nm. In addition, the vibronic maximum of this pyrene based compound is observed at 333 nm.

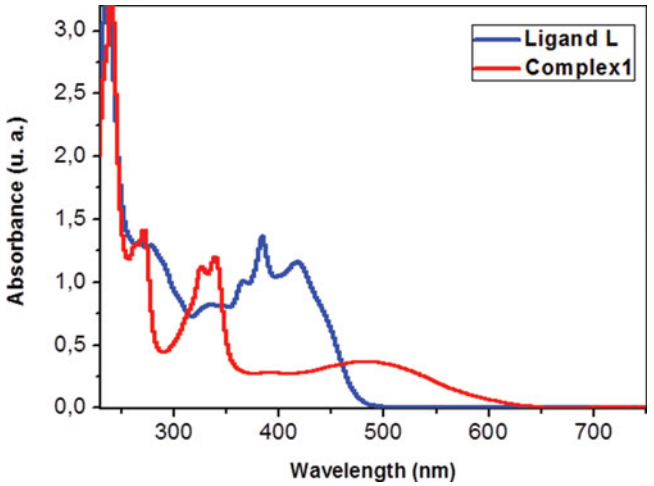

Figure 4. UV-Visible absorption spectra of ligand **L** and complex **1** ($2{\cdot}8{*}10^{-5}$M in dichloromethane at room temperature).

Table 4. Long wavelength absorptions (λ/nm), emission maxima (λ_{em}/nm) and fluorescence quantum yields (Φ_F) of ligand **L** and complex **1** in different solvents and on thin films at 25 °C (λ_{exc} = 317 nm).

	Solvents									
	Methylene chloride			Methanol			Acetonitrile			Thin film
	λ	λ_{em}	Φ_F^a	λ	λ_{em}	Φ_F^a	λ	λ_{em}	Φ_F^a	λ
L	422	414	0.26	416	424	0.004	430	424	0.42	415
1	500	412	0.013	410	428	0.30	415	423	0.024	541

Photophysical parameters are calculated with the formulas: $\tau_f = \Sigma\tau_{f(n)}/n$, $\tau_0 = \tau_f/\Phi_F$, $k_f^r = 1/\tau_0$.

[a] *Fluorescence quantum yields have been calculated with respect to fluorescence emission of pyrene standart* (λ_{exc} = *317 nm*, Φ_F = *0.32, in cyclohexane*.

Upon complexation of the pincer with zinc triflate [$Zn(SCF_3O_3)_2$] the electronic absorption spectrum presents a marked red-shift of long-wavelength absorption maximum from 410 nm in MeOH to 500 nm in CH_2Cl_2. This behavior is ascribed to the strong metal-to-ligand charge transfer (MLCT) occuring in Zn^{2+}/pyrene-pyridine complex structure of **1**. This behavior is decreased in MeOH and Me-CN solutions interacting with the lone-pair electrons of pyridine group resulting the hypsochromic shift.

All fluorescence quantum yields and optical data of ligand **L** and complex **1** are summarized in Table 4. In CH_2Cl_2 solution, ligand **L** and its corresponding zinc complex give emission maxima around 412–414 nm (figure 5), indicating the pyrene monomer emission. It is known that the excimer state of pyrene molecule gives fluorescence at a longer wavelength (between 450 and 520 nm) than the monomer emission [3–14]. A thin layer of the molecules was spin coated at 1500 rpm/s and dried subsequently at 70°C for 20 min on a vacuum controlled etuv. The decay times were detected by the single photon timing method using a laser which has been used to excite the samples at 368 nm. In solid-state film, no clear emission spectrum was observed for the ligand because of its strong quenching process on film state. In fact red-shifted absorption band of the complex is explained by the enhanced MLCT possibility in complex structure reinforcing by double pyrene subunits.

The fluorescence decay times for the studied compounds see table 5 in different solutions (around 4 ns) are not within the lifetime range of excited state of pyrene monomer at about 150–300 ns to generate and stabilize the excimer [15]. The lowest fluorescence quantum yield

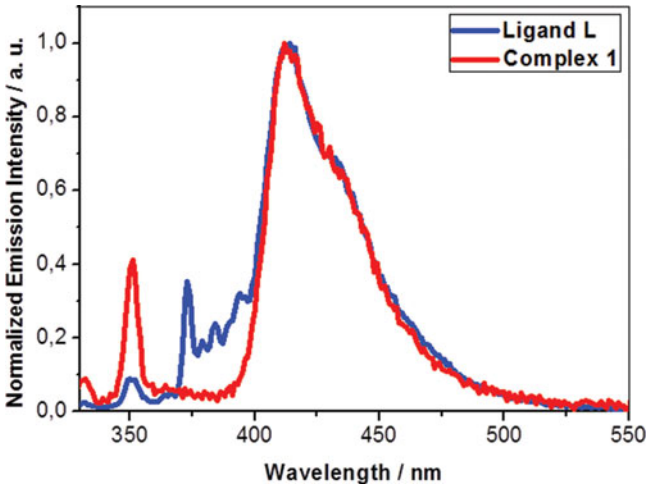

Figure 5. Fluorescence spectra of ligand L and the zinc complex 1 in dichloromethane at room temperature.

Table 5. Fluorescence decay times (τ_f/ns) and their % intensity contributions (given in brackets), radiative lifetimes (τ_0/ns) and fluorescence rate constants ($k_f^r \times 10^7/s^{-1}$) of ligand **L** and complex **1** in different solvents at 25 °C ($\lambda_{exc} = 317$ nm).

	Solvents													
	Methylene chloride					Methanol					Acetonitrile			
	χ^2	$\tau_{f(1)}$	$\tau_{f(2)}$	τ_0	k_f^r	χ^2	$\tau_{f(1)}$	$\tau_{f(2)}$	τ_0	k_f^r	χ^2	τ_f	τ_0	k_f^r
L	1.01	4.30	–	16.5	6.05	0.98	0.56 (9)	4.19 (91)	594	0.17	0.94	4.11	9.8	10.2
1	1.11	4.27	–	328	0.30	0.59	4.23	-	14.1	7.09	1.17	4.15	173	0.58

accompanied with high radiative lifetime around 594 ns and low k_f^r value of 0.17×10^7 s^{-1} is observed for **L** in MeOH solution. This low yield may be explained by the non-fluorescent complex formation between the ground state pyrene monomers. High fluorescence quantum yields and short emission wavelengths below 450 nm for ligand **L**. However, excimer-like interaction arising due to the complex geometry for complex **1** results in the strong quenching of pyrene emission and an decrease of the fluorescence quantum yields below 0.1. For MeOH solution, this is due to the deformation of excimer-like interaction for complex **1** dye in hydrogen bonded methanol solution.

4. Conclusion

In summary, we have synthesized a new pyrene based bisiminopyridine ligand by condensation reaction between 1-aminopyrène and 2,6-pyridinedicarboxaldehyde. The reaction of this ligand with a half equivalent of zinc triflate afforded the a mononuclear complex described by the formula $[Zn(H_2O)LCF_3SO_3)_2].2Et_2O$ **1**. The X-ray structure of this complex indicate a distorted octahedral geometry around the zinc atom and a 3D supramolecular architecture generated *via* hydrogen bonds of type (H···O) and (H···F). The photophysical properties of these compounds have been investigated. Upon complexation a decrease of the monomer emission of pyrene compared with the one of the free ligand is observed.

References

[1] (a) Davis, W.W., Krahl, M.E., & Clowes, G.H.A. (1942). *J. Am. Chem. Sot.*, *64*, 108. (b) Mackay, D., & Shiu, W.Y. (1977). *J. Chem. Eng. Data.*, *22*, 399.

[2] Tsukamoto, T., & Hikida, T. (1996). *J. Photochem. Photobio.*, *95*, 271.

[3] (a) Birks, J. B. (1970). *Photophysics of Aromatic Molecules*; John Wiley: New York, Chapter 7. (b) Winnik, F. M. (1993). *Chem. Rev.*, *93*, 587.

[4] (a) de Silva, A. P., Gunaratne, H. Q. N., Gunnlaugsson, T., Huxley, A. J. M., McCoy, C. P., Rademacher, J. T., & Rice, T. E. (1997). *Chem. Rev.*, *97*, 1515. (b) Rurack, K., & Resch-Genger, U. (2002). *Chem. Soc. Rev.*, *31*, 116.

[5] (a) Simon, J. A., Curry, S. L., Schmehl, R. H., Schatz, T. R., Piotrowiak, P., Jin, X., & Thummel, R. P. (1997). *J. Am. Chem. Soc.*, *119*, 11012. (b) Del Guerzo, A., Leroy, S., Fages, F., & Schmehl, R. H. (2002). *Inorg. Chem.*, *41*, 359. (c) Leroy, S., Soujanya, T., & Fages, F. (2001). *Tetrahedron Lett.*, *42*, 1665. (d) Leroy-Lhez, S., & Fages, F. (2005). *Eur. J. Org. Chem.*, 2684.

[6] (a) Michalec, J. F., Bejune, S. A., & McMillin, D. R. (2000). *Inorg. Chem.*, *39*, 2708. (b) Peng, X., Xu, Y., Sun, S., Wu, Y., & Fan, J. (2007). *Org. Biomol. Chem.*, *5*, 226. (c) Benniston, A. C., Harriman, A., Lawrie, D. J., & Mayeux, A. (2004). *Phys. Chem. Chem. Phys.*, *6*, 51.

[7] Bodenant, B., Fages, F., & Delville, M.-H. (1998). *J. Am. Chem. Soc.*, *120*, 7511.

[8] Harriman, A., Hissler, M., & Ziessel, R. (1999). *Phys. Chem. Chem. Phys.*, *1*, 4203.

[9] Shirase, H., Mori, Y., Fukuda, Y., & Uchiyama, M. (2009). *Monatsh Chem.*, *140*, 801.

[10] (a) Moggia, F., Videlot-Ackermann, C., Ackermann, J., Raynal, P., Brisset, H., & Fages, F. (2006). *J. Mater. Chem*., *16*, 2380. (b) Wu, K.-C., Ku, P.-J., Lin, C.-S., Shih, H.-T., Wu, F.-I., Huang, M.-J., Lin, J.-J., Chen, I.-C., & Cheng, C.-H. (2008). *Adv. Funct. Mater*., *18*, 67. (c) Kwon, J., Hong, J.-P., Lee, S., & Hong, J.-I. (2013). *New J. Chem*., *37*, 2881. (d) Oh, H.-Y., Lee, C., & Lee, S. (2009). *Org. Electron*., *10*, 163. (e) Figueira-Duarte, T. M., & Müllen, K. (2011). *Chem. Rev*., *111*, 7260. (f) Kwon, J., Hong, J.-P., Noh, S., Kim, T.-M., Kim, J.-J., Lee, C., Lee, S., & Hong, J.-I. (2012). *New J. Chem*., *36*, 1813. (g) Mun, J.-W., Cho, I., Lee, D., Yoon, W. S., Kwon, O. K., Lee, C., & Park, S.Y. (2013). *Org. Electron*., *14*, 2341. (h) Lee, O. P., Yiu, A. T., Beaujuge, P. M., Woo, C. H., Holcombe, T. W., Millstone, J. E., Douglas, J. D., Chen, M. S., & Fréchet, J. M. J. (2011). *Adv. Funct. Mater*., *23*, 5359. (i) Kwon, J., Kim, T.-M., Oh, H.-S, Kim, J.-J., & Hong, J.-I. (2014). *RSC Adv*., *4*, 24453.

[11] (a) Britovsek, G.J.P., Gibson, V.C., Kimberley, B.S., Maddox, P.J., McTavish, S.J., Solan, G.A., White, A.J.P., & Williams, D.J. (1998). *Chem. Commun*., 849. (b) Small, B.L., Brookhart, M., & Bennett, A.M.A. (1998). *J. Am. Chem. Soc*., *120*, 4049.

[12] Nita, G., Branzea, D., Pop, F., El-Ghayoury, A., & Avarvari, N. (2012). *Crystals*, *2*, 338.

[13] Sheldrick, G. M. (1996). *Programs for the Refinement of Crystal Structures*, University of Göttingen, Göttingen, Germany.

[14] (a) Nohta, H., Satozono, H., Koiso, K., Yoshida, H., Ishida, J., & Yamaguchi, M. (2000). *Anal. Chem*., *72*, 4199. (b) Jun, E. J., Won, H. N., Kim, J. S., Lee, K.-H., & Yoon, J. (2006). *Tetrahedron Lett*., *47*, 4577.

[15] Snare, M. J., Thistlethwaite, P. J., & Ghiggino, K. P. (1983). *J. Am. Chem. Soc*., *105*, 3328.